10-7-2011

Axl2 Integrates Polarity Establishment, Maintenance, and Environmental Stress Response in the Filamentous Fungus Ashbya Gossypii

Jonathan F. Anker
Dartmouth College

Amy S. Gladfelter
Dartmouth College

EUKARYOTIC CELL, Dec. 2011, p. 1679–1693 Vol. 10, No. 12
1535-9778/11/$12.00 doi:10.1128/EC.05183-11

Axl2 Integrates Polarity Establishment, Maintenance, and Environmental Stress Response in the Filamentous Fungus *Ashbya gossypii*▽†

Jonathan F. Anker and Amy S. Gladfelter*

Department of Biological Sciences, Dartmouth College, Hanover, New Hampshire 03755

Received 26 July 2011/Accepted 2 October 2011

In budding yeast, new sites of polarity are chosen with each cell cycle and polarization is transient. In filamentous fungi, sites of polarity persist for extended periods of growth and new polarity sites can be established while existing sites are maintained. How the polarity establishment machinery functions in these distinct growth forms found in fungi is still not well understood. We have examined the function of Axl2, a transmembrane bud site selection protein discovered in *Saccharomyces cerevisiae*, in the filamentous fungus *Ashbya gossypii*. *A. gossypii* does not divide by budding and instead exhibits persistent highly polarized growth, and multiple axes of polarity coexist in one cell. *A. gossypii axl2*Δ (Ag*axl2*Δ) cells have wavy hyphae, bulbous tips, and a high frequency of branch initiations that fail to elongate, indicative of a polarity maintenance defect. Mutant colonies also have significantly lower radial growth and hyphal tip elongation speeds than wild-type colonies, and Ag*axl2*Δ hyphae have depolarized actin patches. Consistent with a function in polarity, AgAxl2 localizes to hyphal tips, branches, and septin rings. Unlike *S. cerevisiae* Axl2, AgAxl2 contains a Mid2 homology domain and may function to sense or respond to environmental stress. In support of this idea, hyphae lacking AgAxl2 also display hypersensitivity to heat, osmotic, and cell wall stresses. Axl2 serves to integrate polarity establishment, polarity maintenance, and environmental stress response for optimal polarized growth in *A. gossypii*.

The establishment and maintenance of cell polarity are essential for proper cell morphology and growth in both unicellular and multicellular eukaryotes (25, 39). Directional growth, neuronal development and function, membrane trafficking in epithelial cells, and whole-cell motility by chemotaxis all rely on the generation of cell polarity (5, 88, 97). Polar growth has been linked to fungal virulence in human pathogens such as *Candida albicans*, *Aspergillus fumigatus*, *Cryptococcus neoformans*, and *Paracoccidioides brasiliensis* (3, 6, 67, 80). Many mechanisms governing cell polarity and polarized growth were discovered in the budding yeast, *Saccharomyces cerevisiae*, and are highly conserved from unicellular eukaryotes to humans (62).

In *S. cerevisiae*, budding can occur in either an axial or a bipolar manner, which is determined by specific landmark proteins. The axial landmark consists of the septin complex, *S. cerevisiae* Bud3 (ScBud3), ScBud4, ScAxl1, and ScAxl2 and functions by recruiting members of the Cdc42 signaling pathway (1, 14, 30, 31, 38, 44, 45, 69, 72, 98). The localization and activation of Cdc42 at sites specified by the landmarks then direct bud formation through polarization of the actin cytoskeleton (2, 99). Polarized actin cables form tracks on which myosins transport secretory vesicles to the growing bud (11, 29, 37). Polarized cortical actin patches are sites of endocytosis and as such can function to internalize any polarity factors that diffuse beyond the region of polarized growth (36, 57, 61).

ScAxl2 was identified in a screen for multicopy suppressors of *spa2*Δ *cdc10-10* lethality and for mutants no longer able to undergo axial budding (38, 69). ScAxl2 is a type I integral plasma membrane protein containing an N-linked glycosylated extracellular N-terminal domain rich in serines and threonines, a transmembrane domain, and an intracellular C-terminal domain (38, 69). In addition, ScAxl2 contains O-linked glycosylations, dependent on ScPmt4, which are important for its stability and localization (73). ScAxl2 also contains four cadherin-like motifs in its extracellular domain whose functions remain unknown (23). Individual deletions of Sc*BUD3*, Sc*BUD4*, Sc*AXL1*, and Sc*AXL2* all resulted in a switch from axial to bipolar budding (32, 38, 55, 69). The additional deletion of Sc*RAX1*, a bipolar bud site selection landmark, caused cells also lacking ScBud3, ScBud4, or ScAxl1 to revert back to axial budding, while cells deleted for both Sc*RAX1* and Sc*AXL2* bud randomly, indicating that ScAxl2 is the true axial landmark protein (32, 55).

ScAxl2 may play an additional role in polarized growth, independent of its role as an axial landmark. The expression of ScBud3 and ScBud4 peaks from S phase to mitosis, while ScAxl2 expression peaks during late G_1 (16, 56, 78). Additionally, while ScBud3 and ScBud4 are recruited to the bud neck by septins, ScAxl2 has diverse localizations during the cell cycle, including at the bud tip and bud neck (14, 38, 69, 72). In the absence of the protein ScErv14, ScAxl2 localization to the cell surface is lost, and these mutant cells experience polarized growth defects (65, 66). In addition, unlike multicopy ScBud3p, ScBud4p, and ScAxl1p, multicopy ScAxl2 is able to suppress an

* Corresponding author. Mailing address: Department of Biological Sciences, Dartmouth College, Hanover, NH 03755. Phone: (603) 646-8706. E-mail: amy.gladfelter@dartmouth.edu.

† Supplemental material for this article may be found at http://ec.asm.org/.

▽ Published ahead of print on 7 October 2011.

TABLE 1. *Ashbya gossypii* strains

Strain	Genotype	Parent strain	Reference
Wild type	Δ*leu2*Δ*thr4* (Δ*l*Δ*t*)		3a
AG127	*SEP7-GFP-NAT1* Δ*l*Δ*t*	Wild type	21
AG124	*SEP7-GFP-GEN3* Δ*l*Δ*t*	Wild type	21
AG379.5	*axl2*Δ::*GEN3 SEP7-GFP-NAT1* Δ*l*Δ*t*	AG127	This study
AG230	*CDC11a-mCherry-NAT1* Δ*l*Δ*t*	Wild type	21
AG527	*AXL2-GFP-GEN3 CDC11a-mCherry-NAT1* Δ*l*Δ*t*	AG230	This study
AG528.3	*AXL2-6HA-GEN3 CDC11a-mCherry-NAT1* Δ*l*Δ*t*	AG230	This study

ScCdc42 mutant phenotype (33). The first third of ScAxl2's intracellular tail is able to interact with polarity proteins ScCdc42, ScBem1, and ScCdc24, and this region alone is sufficient both to suppress the ScCdc42 mutant phenotype and to localize ScAxl2 to regions of polarized growth, but not to the bud neck (33). Final evidence for ScAxl2's involvement in polar growth is that ScAxl2, in addition to ScCdc42 but unlike the other axial landmark proteins, was identified as a multicopy suppressor of cells lacking both polarity proteins ScRho3 and ScRho4 (58). Precisely how Axl2 contributes to polar growth and if this is a conserved function is not known.

A third role for ScAxl2 lies in regulating septin organization. The septins are a conserved family of GTP-binding proteins that, in addition to acting as axial budding landmarks, function in processes such as cytokinesis, membrane remodeling, and exocytosis and as signaling scaffolds and diffusion barriers (7, 27, 28, 35, 46, 81, 85, 89). In addition, altered expression and activity of septins have been linked to cancer, neurodegenerative disorders, and fungal virulence (13, 15, 47, 87). Sc*axl2*Δ mutants have elongated bud necks, short chains of cells, and asymmetrically "droopy" buds, all consistent with a possible septin defect (69). In addition, multicopy ScAxl2 suppresses the elongated bud and septin defect phenotype of a partial-loss-of-function ScCdc42 mutant with septin defects (12, 33). Although cells lacking ScAxl2 do not display obvious septin defects, cells missing both ScAxl2 and either ScGin4, ScCla4, or ScElm1, all known septin regulators, display severe septin disorganization and defective ring assembly (9, 18, 54, 69, 84, 90).

While budding yeast has been essential for the discovery of fundamental polarity mechanisms and proteins, yeast cells' polarized growth period is transient such that the polarity site is lost with each cell cycle. Budding yeast, therefore, does not serve as an ideal system in which to study highly polarized growth or understand how multiple polarity sites may coexist. One such model system is the highly polarized *Ashbya gossypii*, which grows through the elongation of constantly polarized hyphae and the generation of new hyphae through lateral branching and is not known to ever divide by budding (4, 48, 94). Despite the morphological differences between *S. cerevisiae* and *A. gossypii*, over 95% of all *A. gossypii* genes, including the bud site selection machinery genes, have a homologue within the *S. cerevisiae* genome (10, 24).

We demonstrate here that *A. gossypii* Axl2 (AgAxl2) (which will be referred to as Axl2) plays an important role in maintaining the highly polarized and persistent growth of hyphae, in creating new stable axes of polarized growth with lateral branches, and in enabling cells to respond to environmental stress. We present a model in which Axl2 coordinates the extracellular status of the cell wall with intracellular morphogenesis programs.

MATERIALS AND METHODS

Strain construction. Strains used and created are listed in Table 1, and plasmids used for creating these strains are listed in Table S1 in the supplemental material. The BglI restriction enzyme and buffer used in this study were from New England BioLabs (Beverly, MA), and PCR was performed using reagents from Roche Diagnostics (Indianapolis, IN) and New England BioLabs. Oligonucleotides used are listed in Table S2 in the supplemental material, and those designed in this study were synthesized by Integrated DNA Technologies (Coralville, IA). PCR band gel extraction, plasmid minipreparations, and isolation of genomic DNA were performed using kits from Qiagen (Germantown, MD).

To create strain AG379.5 (*axl2*Δ::*GEN3 SEP7-GFP-NAT1* Δ*l*Δ*t*), plasmid AGB021 was digested with BglI and the sequence containing the G418 resistance gene, *GEN3*, was gel purified. *GEN3* was then amplified using primers AGO529 and AGO530, which contain ~20 bp of homology to the termini of *GEN3* and ~45 bp of homology to the termini of genomic *AXL2*. The amplified marker was transformed by electroporation into strain AG127 to allow for *GEN3* integration and *AXL2* deletion to occur by homologous recombination (92). Transformants were grown on *Ashbya* full medium (AFM) agarose plates containing G418 (200 μg/ml). These transformants were heterokaryons, as not all nuclei of the multinucleated cells underwent successful recombination. To isolate homokaryons, in which all nuclei of the cells contain the targeted genetic manipulation, individual spores were isolated and grown on AFM agarose plates containing G418. Homokaryon strains were verified by PCR using primers AGO531, AGO532, AGO533, AGO36, and AGO37. Mycelial stocks were created using 75% AFM and 25% glycerol and were stored at −80°C for >3 individual transformants. Experiments were performed on two independent transformants. Spore stocks were generated using either Sigmacote-coated tubes, which isolate spores based on their hydrophobicity, or Zymolyase 20T, which digests the cell wall and releases spores, and were stored at −80°C.

To create strain AG527 (*AXL2-GFP-GEN3 CDC11a-mCherry-NAT1* Δ*l*Δ*t*), plasmid AGB005 was digested using BglI and the sequence carrying both *GFP* and *GEN3* was gel purified. *GFP-GEN3* was then amplified using primers AGO1023 and AGO1024, which contain ~20 bp of homology to the termini of the *GFP-GEN3* sequence, 24 bp carrying alternating alanine and glycine codons to act as a linker region between the protein and the tag, and ~45 bp of homology beginning either at the stop codon of *AXL2* or shortly downstream. The amplified sequence was transformed into strain AG230, and transformants were selected for on AFM agarose plates containing G418 (200 μg/ml). Expression of Axl2-GFP was verified by microscopy, and integration was verified by PCR using primers AGO532, AGO917, AGO94, and AGO95.

To create strain AG528.3 (*AXL2-6HA-GEN3 CDC11a-mCherry-NAT1* Δ*l*Δ*t*), the procedure followed to create strain AG527 was repeated, using primers AGO1022 and AGO1024, which contain ~20 bp of homology to the termini of the *6HA-GEN3* sequence on plasmid AGB035, 24 bp carrying alternating alanine and glycine codons to act as a linker region between the protein and the tag, and ~45 bp of homology beginning either at the stop codon of *AXL2* or shortly downstream. The amplified sequence was transformed into strain AG230, and transformants were selected for on AFM agarose plates containing G418 (200 μg/ml). Expression of Axl2-6HA was verified by microscopy.

Growth conditions. For microscopic analysis, *A. gossypii* spore stocks were incubated in liquid AFM and ampicillin (1 μl/ml) for 15 to 16 h with shaking at 30°C. Cells were exposed to treatments of Echinacea (Nature's Answers, Hauppauge, NY), calcofluor white (Sigma-Aldrich, St. Louis, MO), Congo red (Sigma-Aldrich), caffeine (Sigma-Aldrich), NaCl (Fischer Scientific, Fair Lawn,

NJ), rapamycin (LC Laboratories, Woburn, MA), and heat (37°C) for the full 15 to 16 h growth period.

For radial growth analysis, *axl2*Δ and wild-type mycelia were grown on AFM agarose plates containing G418 (200 μg/ml). After 3 days, a measured circular area of biomass was transferred to AFM agarose plates containing ampicillin (100 μg/ml) and none or one of the above-described treatments, allowing for all plates to contain an equivalent concentration of mycelia on day 0 of surface area quantification. All treatments were added directly to agarose plates, except rapamycin (LC Laboratories, Woburn, MA), which was taken from a 1-mg/ml stock in 90% ethanol (EtOH) and 10% Tween 20 (53). All plates, other than those at 37°C and room temperature, were incubated at 30°C. Quantification of surface area was performed using an ImageJ macro to identify colony boundaries through image thresholding.

For branching-frequency assays and morphological analysis, cells were fixed with 2% paraformaldehyde, washed twice with 1× phosphate-buffered saline (PBS), and mounted on a glass slide with mounting medium for visualization. Still-image snapshots and three-dimensional (3-D) Z stacks were analyzed using Volocity (Improvision-Perkin-Elmer), and branch initiations were determined by analyzing individual planes in Z stacks of phase-contrast images.

For hyphal tip growth speed analysis, spores were grown either on a medium-containing solid agarose gel pad overnight or in liquid AFM and ampicillin (1 μg/ml) overnight and transferred to a gel pad 30 min before imaging. Gel pads contained 25% AFM and 75% low-fluorescence minimal medium. Time-lapse microscopy was performed in a temperature-controlled chamber at the specified temperatures. Hyphal tip growth speed quantification was performed using Volocity, tracking the positions of individual hyphae over 5-min intervals and controlling for overall cell positioning.

Statistical significance was determined using two-sample *t* tests with two-tailed distribution.

Visualization of F-actin. To visualize the actin cytoskeleton, cells were fixed with 3.7% formaldehyde and 10% Triton for 10 min in the dark, followed by centrifugation, resuspension in 1× PBS, and a second fixation in 3.7% formaldehyde for 1 h in the dark. The cells were then centrifuged and washed with and resuspended in 1× PBS, followed by a 1-h dark incubation with Alexa Fluor 568 phalloidin (Invitrogen). After staining, cells were washed twice with 1× PBS and mounted on a glass slide with mounting medium for visualization. Fluorescent images were acquired using identical exposure settings, and images were normalized and contrasted to equivalent levels set at an identical white point and black point. Tip fluorescence quantification was performed using Volocity, measuring the sum fluorescence within an equivalent circular area at hyphal tips.

FM4-64FX. FM4-64FX (Molecular Probes) was used to analyze endocytosis. Cells were grown for 16 h with shaking at 30°C. Cells were then exposed to FM4-64FX at a final concentration of 2 μM for 5 or 15 min, followed by fixation with 2% paraformaldehyde and visualization by fluorescence microscopy.

Immunofluorescence. To visualize Axl2-6HA and Cdc11-mCherry, cells were fixed in 3.7% formaldehyde for 1 h, centrifuged, washed once in 1× PBS, centrifuged, resuspended in solution A (0.1 M potassium phosphate buffer [pH 7.5], 1.2 M sorbitol, H_2O), and digested with 15-mg/ml Zymolyase with rotating at 37°C until cells were phase dark. Cells were lightly washed twice with solution A and added to polylysine-treated wells. Cells were washed twice with 1× PBS and then blocked by treatment with 1× PBS plus 1 mg/ml bovine serum albumin (BSA) for 30 min. Cells were incubated with a 1/50 dilution of primary monoclonal mouse antihemagglutinin (anti-HA) (Covance) and primary polyclonal rabbit anti-Cdc11 antibodies (Santa Cruz) overnight in a humid chamber at 4°C. Cells were then washed 10 times in 1× PBS plus BSA, followed by incubation with a 1/200 dilution of secondary Alexa Fluor 488 goat anti-mouse and Alexa Fluor 568 goat anti-rabbit antibodies (Invitrogen) for 2 h in a humid chamber at room temperature. Cells were then washed 10 times with 1× PBS plus BSA, and the slide was mounted with mounting medium and sealed.

Microscopy. Images were acquired using an AxioImager-M1 wide-field upright light microscope (Carl Zeiss, Jena, Germany) equipped with Zeiss EC Plan-Neofluar 40×/1.3 numerical aperture and Zeiss EC Plan-Apochromat 63×/1.4 numerical aperture oil immersion objectives. Green fluorescent protein (GFP) and mCherry fluorophores were visualized using the filter sets 38HE (Carl Zeiss) and 41043 (Chroma Technology, Brattleboro, VT), respectively. Alexa Fluor 568 phalloidin was visualized using the filter set 41002B (Chroma Technology). An Exfo X-Cite 120 lamp was used for the fluorescence light source, and an Orca-AG (C4742-80-12AG; Hamamatsu, Bridgewater, NJ) charge-coupled device camera was utilized for image acquisition with Volocity. Z stacks of still images were acquired at 0.5-μm slices for fixed imaging and 0.75-μm slices for time-lapse imaging, and fluorescent image stacks were processed by fast or iterative deconvolution using calculated point spread functions.

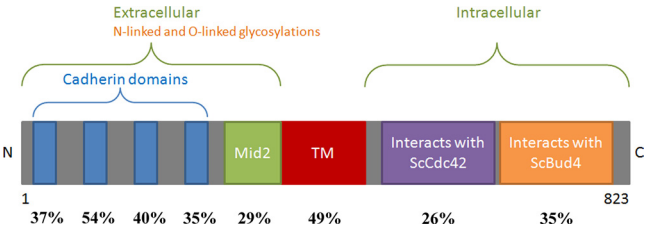

FIG. 1. Genetic conservation between *S. cerevisiae* and *A. gossypii* Axl2 homologues. Axl2 domains share a high degree of aligned sequence conservation between *S. cerevisiae* and *A. gossypii*. Percentages were quantified for aligned identical amino acid matches between the AgAxl2 sequence and the known cadherin-like domains and transmembrane domain of ScAxl2, the regions of ScAxl2 that are able to interact with ScCdc42 and ScBud4, and the region of ScAxl2 that aligns with the ScMid2 homology domain within AgAxl2.

RESULTS

Axl2 conservation and deletion strategy in *A. gossypii*. We hypothesized that proteins that function in bud site selection in yeasts may be an important link between septins, the plasma membrane, and the hyphal tip in filamentous fungi. Axl2 in *A. gossypii* is a syntenic homologue of ScAxl2. The two proteins display a high degree of conserved sequence alignment (ClustalX2, GeneDoc), including within the known ScAxl2 domains. ScAxl2 contains four putative cadherin-like domains, which, from the N terminus to the C terminus, contain 37%, 54%, 40%, and 35% conservation of identical aligned amino acids between ScAxl2 (822 amino acids) and AgAxl2 (831 amino acids) over a length of 428 amino acids. Both homologues are type I transmembrane proteins, with a predicted extracellular N terminus and intracellular C terminus and a single transmembrane domain with 49% sequence conservation. The first third of the intracellular domain of ScAxl2 is able to interact with ScCdc42, and the middle region of the intracellular domain is able to interact with ScBud4 and is necessary for axial budding and bud neck ScAxl2 localization, and these domains contain 26% and 35% aligned sequence conservation, respectively, between budding yeast and the filamentous fungus (Fig. 1). Interestingly, there is an additional sequence in the extracellular portion of AgAxl2 that contains a conserved domain of ScMid2, a protein that is required for stress response in the budding yeast (64, 68). AgAxl2 has 29% conserved homology with ScAxl2 within this region. Additionally, the predicted Axl2 homologue within the filamentous fungi *Neurospora crassa*, *Aspergillus nidulans*, and *Candida albicans* contain 20.6%, 11.8%, and 26.5% conservation, respectively, with AgAxl2 within this ScMid2 homology region. Thus, there is some minimal homology in domains of Axl2 that are implicated in morphogenesis that are conserved between these distant species and a novel region of the AgAxl2 homologue that could function in environmental sensing in filamentous fungi.

***axl2*Δ cells display a defect in polarized cell growth.** In order to analyze Axl2 function in *A. gossypii*, we used a PCR-based gene targeting approach to delete the *AXL2* open reading frame (ORF) from the *A. gossypii* genome. We successfully generated and verified *A. gossypii axl2*Δ homokaryon strains, in which *AXL2* was removed from all nuclei of the multinucleated cells. *axl2*Δ cells expressing the septin Shs1-GFP were fixed, so

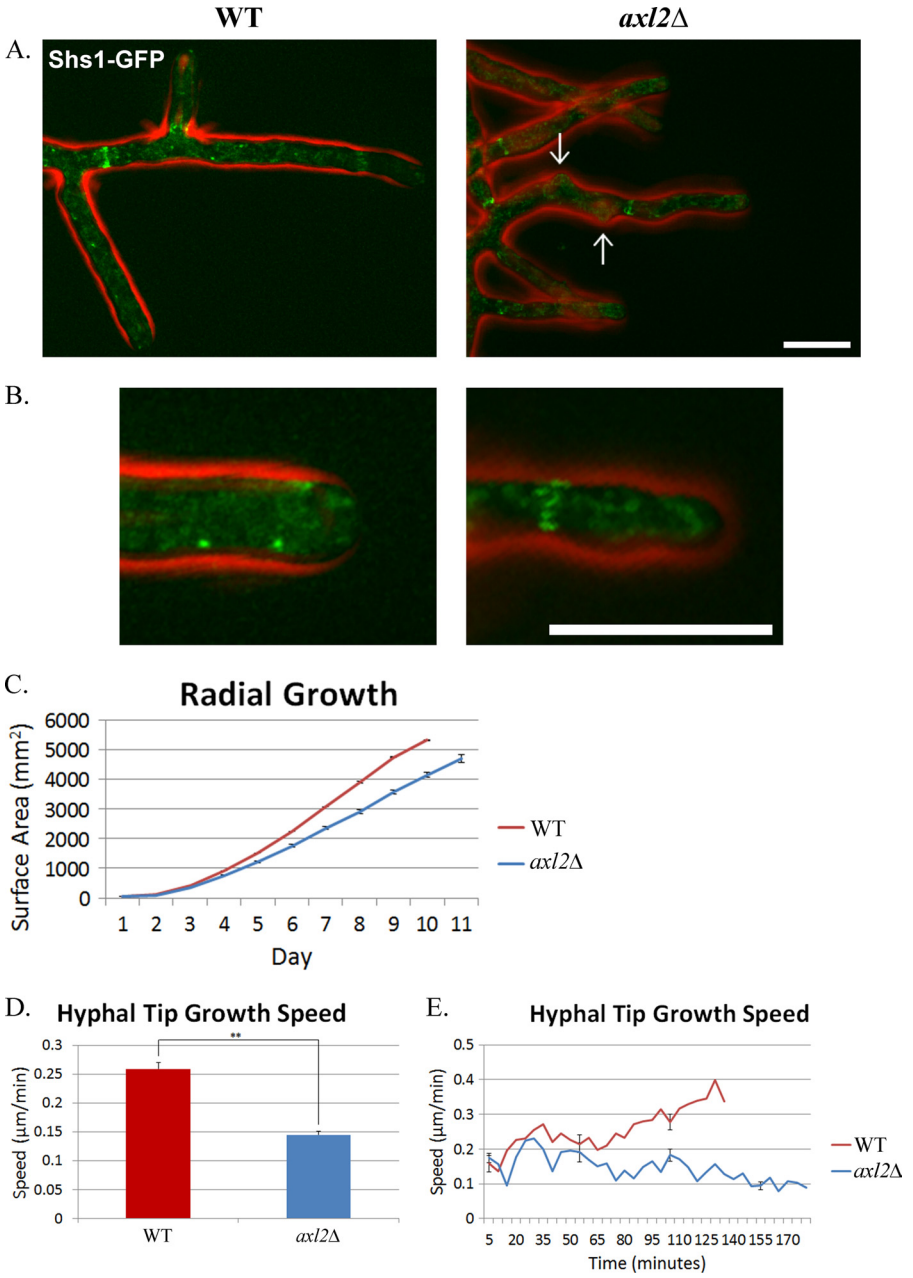

FIG. 2. *axl2*Δ cells and colonies exhibit polarized growth defects. (A and B) Cells were imaged after growth at 30°C for 15 h and fixation with 2% paraformaldehyde. Arrows indicate nascent branches. Bars are 10 μm. (C) Equal concentrations of mycelia were transferred to 85-mm-diameter AFM agarose plates, and mycelium surface areas were measured every 24 h. (D and E) Live, growing hyphae of single cells were imaged by time-lapse microscopy every 5 min on medium-containing agarose gel pads. Wild type (WT), $n = 5$ to 13 hyphal tips per time point; *axl2*Δ mutant, $n = 6$ to 8 hyphal tips per time point. Wild type, $n = 27$ time points; *axl2*Δ mutant, $n = 36$ time points. Error bars denote standard errors. Statistical significance was determined using two-sample *t* tests with a two-tailed distribution. **, $P < 0.001$.

as to preserve GFP, and visualized by fluorescence microscopy. Remarkably, the septin cortex did not display any severe defects. Interregion septin rings, located throughout the hyphae, were cortically assembled in a normal frequency and appearance, and septins were present at the bases of all branches (Fig. 2A). In addition, *axl2*Δ spores were able to germinate, initiate and maintain polarized hyphal growth, and undergo lateral branching. However, some *axl2*Δ cells exhibited curved hyphae with an increase in short, immature branches (see Fig. 3 for quantification), in contrast to the straight hyphae and developed branches seen in the wild-type parent strain (Fig. 2A). In addition, some *axl2*Δ hyphal tips appeared to be slightly deformed and bulbous (Fig. 2B). This phenotype is indicative of a possible polarity maintenance defect.

In order to determine if these subtle morphological defects were affecting growth rate, we measured the radial growth of *axl2*Δ and wild-type colonies. After 8 days of growth on plates, the *axl2*Δ colony surface area (3,565 mm^2, standard error

[SE] = 72 mm^2, $n = 3$) and growth rate were reduced by 25% compared to those of wild-type colonies (4,743 mm^2, SE = 4.1 mm^2, $n = 3$) ($P < 0.003$) (Fig. 2C). Thus, Axl2 is required for maximum growth on the colony level.

In order to determine the cause of the decreased radial growth of *axl2*Δ colonies, we performed live, single-cell time-lapse microscopy, acquiring stacks of images every 5 min of individual hyphae growing on medium-containing agarose gel pads. The average elongation speed of *axl2*Δ hyphal tips was 8.4 μm/h (SE = 0.39 μm/h, $n = 36$ time points, 8 hyphal tips), 44.0% slower than the average speed of wild-type hyphae, at 15.6 μm/h (SE = 0.72 μm/h, $n = 27$ time points, 13 hyphal tips) ($P < 0.001$) (Fig. 2D). Hyphal tip growth speed is known to steadily increase over time, as an increasing number of vesicles are continually incorporated into the growing tip (48, 49, 74). In agreement, the average hyphal tip growth speeds over 5-min intervals revealed that wild-type tips gradually increased growth speed over time. However, *axl2*Δ hyphae did not display an increase in tip growth speed, and elongation rates remained relatively constant over time (Fig. 2E). These data provide evidence that Axl2 plays a role in maintaining efficient tip elongation and growth acceleration.

Axl2 plays a role in lateral branching. In addition to a marked reduction in colony expansion, *axl2*Δ colonies also were more transparent than wild-type colonies, suggesting that there may be less biomass (Fig. 3A). To determine if in fact there was a change in the colony density (biomass over a surface area), we weighed the mycelia of each plate and normalized each weight by the surface area of those mycelia. a*xl2*Δ colonies had a density of 0.195 mg/mm^2 (SE = 0.01 mg/mm^2, $n = 3$), which is 50.2% less lower than that of wild-type colonies, at 0.391 mg/mm^2 (SE = 0.006 mg/mm^2, $n = 3$) ($P < 0.001$) (Fig. 3B).

While the decrease in *axl2*Δ hyphal tip growth speed can explain the radial growth rate defect and the aberrant hyphal morphology, it does not explain the significant decrease in cell density of *axl2*Δ mycelia. Initial single-cell imaging, however, suggested that there were many short branches in even young cells. To evaluate whether lateral branching was altered in the *axl2*Δ mutants, we quantified the hyphal distance between branch sites emerging along wild-type and *axl2*Δ hyphae. The average distance between branches in wild-type cells was 8.12 μm (SE = 0.31 μm, $n = 151$). Surprisingly, branching frequency increased 32.6% along *axl2*Δ hyphae, which displayed an average interbranch distance of 5.48 μm (SE = 0.19 μm, $n = 190$) ($P < 0.001$) (Fig. 3C). However, these branches failed to persist and elongate, and 30.0% of *axl2*Δ branches were under 2 μm in length, in contrast to only 4.6% of wild-type branches (Fig. 3D). The decreased density of *axl2*Δ colonies is likely caused by many lateral branches that initiated but failed to grow.

***axl2*Δ cells have depolarized F-actin patches.** The F-actin cytoskeleton is permanently polarized at growing tips to support hyphal growth, and new sites of F-actin polarization arise for lateral branch emergence. To determine whether the *axl2*Δ growth defects resulted from actin cytoskeletal depolarization, we visualized F-actin in *axl2*Δ and wild-type cells using fluorescently labeled phalloidin. Wild-type cells have F-actin cables aligned parallel to the growth axis emanating from tips, and patches are concentrated at the tips. In contrast, while cables were polarized in *axl2*Δ cells, cortical actin patches were depolarized from hyphal tips (Fig. 4A), generating a 37.3% decrease in total fluorescence compared to that of wild-type tips (*axl2*Δ, $n = 170$ tips; wild type, $n = 145$ tips) ($P < 0.001$) (Fig. 4B). We cannot rule out the presence of a subtle cable defect, but the primary problem with F-actin organization is visible in patch localization. The *axl2*Δ cortical actin patch depolarization may be the direct cause of the decreased hyphal tip growth speed and the inability to maintain polarized growth in newly formed branches.

Actin patches are sites of endocytosis in yeast cells (36, 57, 61), and therefore we assessed whether the depolarized actin patches in *axl2*Δ cells were associated with a diminished capacity for endocytosis. We used the fluorescent lipophilic styryl dye FM4-64FX to visualize endocytosis within hyphae (Fig. 5). Wild-type hyphae displayed what is likely vacuolar, endosome, and plasma membrane staining, while *axl2*Δ hyphae displayed much smaller cortical intermediates, similar to those seen in *S. cerevisiae* deleted for the endocytic proteins ScShe4, ScPan1, and ScEnd3 or subjected to ethanol stress or heat shock (59, 91). Therefore, defective patch polarity may be leading to inefficient endocytosis which leads to defects in polarity maintenance in *axl2*Δ cells.

***axl2*Δ cells are hypersensitive to environmental stress.** The F-actin cytoskeleton is known to depolarize in *S. cerevisiae* in response to heat shock, osmotic shock, and cell wall stress (17, 22, 52, 57) and in *A. gossypii* in response to heat (21). In addition, AgAxl2 contains a potential Mid2 family domain in its extracellular tail that is not present in the budding yeast homologue. ScMid2 is a type 1 membrane protein with a serine- and threonine-rich extracellular N terminus that acts as a sensor of environmental stress and is able to respond by signaling through ScRom2, the ScRho1 guanine nucleotide exchange factor (GEF), to lead to cell wall remodeling (43, 64, 68). ScAxl2 also contains both N-linked and O-linked glycosylations, signifying a potential physical interaction with the cell wall (38, 69, 73). To determine if the *axl2*Δ mutant has an increased sensitivity to environmental stress, we exposed *axl2*Δ and wild-type cells to 37°C heat stress, a 0.2 M NaCl hypertonic medium, and the cell wall stressors Congo red and caffeine.

Growth in 0.2 M NaCl caused severe morphological defects in *axl2*Δ cells that were not seen in wild-type cells. After osmotic stress, *axl2*Δ hyphae became extremely wavy and displayed deformed, thick hyphae containing tight constrictions, many failed branches, and spherical, bulbous tips (Fig. 6A), seemingly an exacerbation of the *axl2*Δ phenotype under no stress (Fig. 2A and B). After growth at 37°C, the subtle *axl2*Δ phenotype of wavy hyphae and short immature branches was readily apparent. Additionally, spherical cell extensions were visible emanating from hyphal tips and some septa of *axl2*Δ cells fixed after growth at 37°C (Fig. 6B). These spherical protrusions may represent a cell wall sensitivity, as these cell walls are potentially failing to undergo proper preservation and stable protein cross-linking during fixation with paraformaldehyde. After exposure to the cell wall stressors Congo red and caffeine, *axl2*Δ cells again displayed wavy tree-like hyphae, containing many closely initiated but immature branches (Fig. 6C and D). While the more morphologically disturbed *axl2*Δ hyphae do not display visible septin rings, proper septin assembly and organization were observed within the populations of

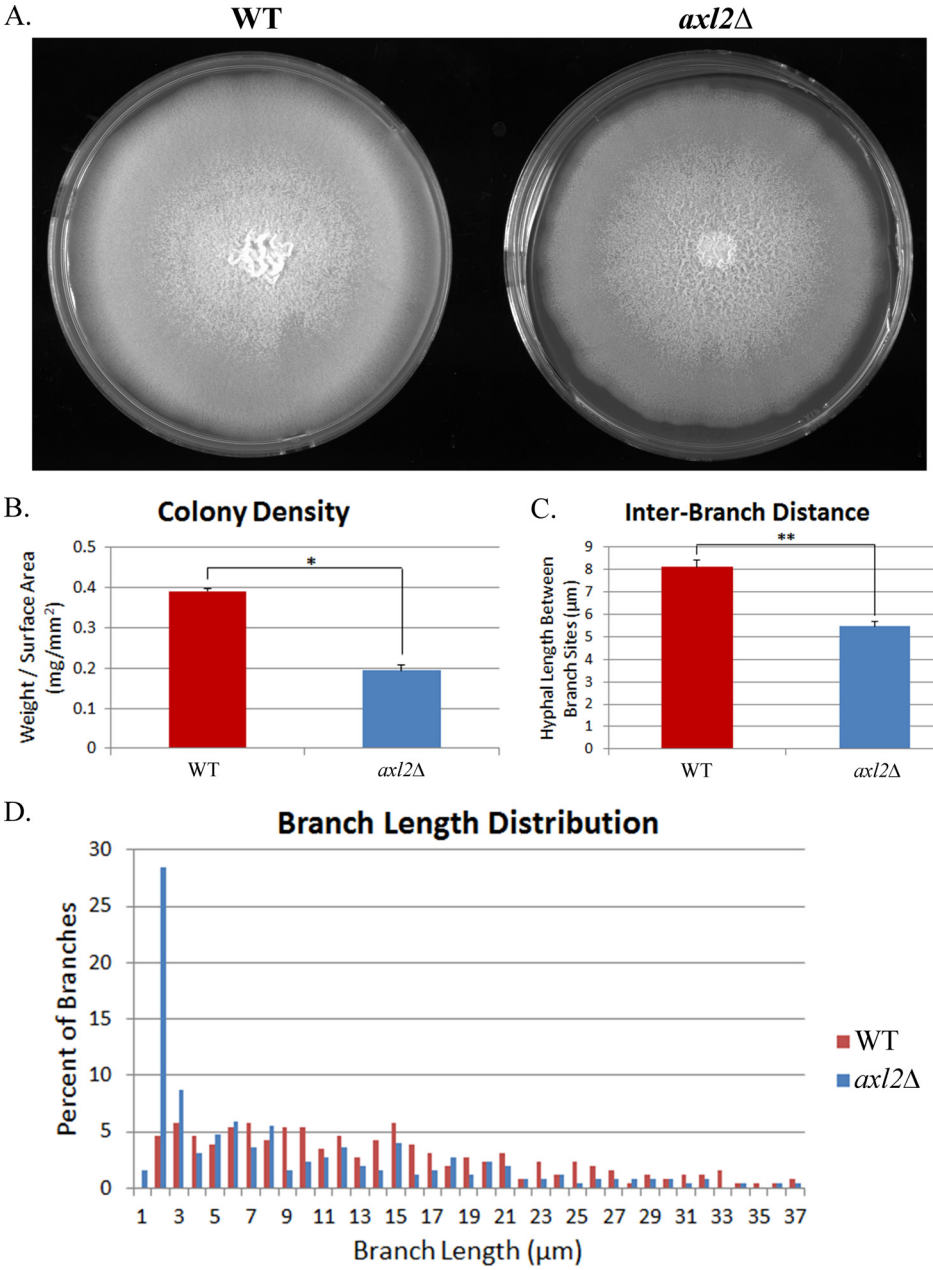

FIG. 3. *axl2*Δ colonies are less dense and contain more frequent, short branches. (A and B) After maximal growth, colonies were imaged (A) and colony density was determined by colony weight divided by surface area (B). Density assays were repeated 3 independent times for each strain. (C) Cells were grown for 15 h at 30°C and imaged after fixation with 2% paraformaldehyde. The interbranch distance was quantified as the hyphal length between branch sites. Wild type, $n = 151$ interbranch measurements; *axl2*Δ mutant, $n = 190$ interbranch measurements. (D) Branch lengths were quantified from the branch base to the hyphal tip. Wild type, $n = 262$ branch lengths; *axl2*Δ mutant, $n = 253$ branch lengths. Error bars denote standard errors. Statistical significance was determined using two-sample *t* tests with a two-tailed distribution. *, $P < 0.05$; **, $P < 0.001$.

both *axl2*Δ and wild-type cells after exposure to all stressors, suggesting that septin ring assembly is not as sensitive to these stresses as cell polarity.

To determine the functional implications of these morphogenesis phenotypes and of the *axl2*Δ mutant's sensitivity to environmental stress, we performed a radial growth assay of *axl2*Δ and wild-type mycelia growing on plates containing different environmental stressors (Fig. 7A). The cell wall stressors utilized were Echinacea, calcofluor white, Congo red, and caffeine. Echinacea is a natural herb used as an antifungal treatment and is thought to target the fungal cell wall (60, 76). Congo red binds to and disrupts the cell wall by inhibiting β-1,3-glucan assembly within the cell wall, and calcofluor white disrupts chitin synthesis and is able to bind chitin and inhibit the assembly of chitin fibrils within the cell wall (26, 40, 50, 70, 71). Caffeine activates the Pkc1-mitogen-activated protein ki-

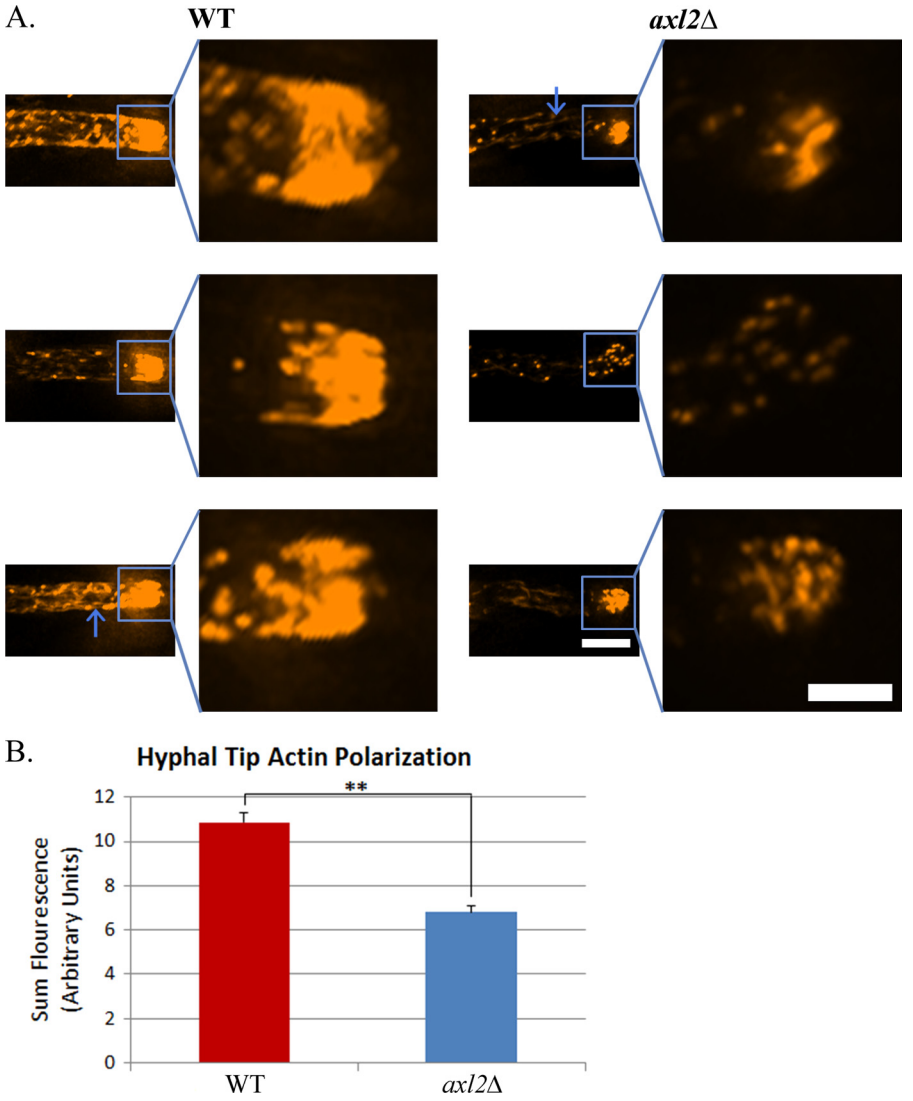

FIG. 4. The *axl2*Δ actin cytoskeleton is depolarized from hyphal tips. (A) Cells were grown for 16 h at 30°C and imaged after fixation with 3.7% formaldehyde and actin staining with Alexa Fluor 568 phalloidin. Images of actin fluorescence within hyphae were normalized and contrasted to equivalent levels. Tips were magnified, and actin fluorescence tip images were normalized and contrasted to equivalent levels. Arrows indicate a polarized actin cable. Hypha image bars are 5 μm, and tip image bars are 2 μm. (B) Sum fluorescence was quantified over an equivalent circular area at hyphal tips. Error bars denote standard errors. Wild type, $n = 145$ tips; *axl2*Δ mutant, $n = 170$ tips. Statistical significance was determined using two-sample t tests with a two-tailed distribution. **, $P < 0.001$.

nase (MAPK) cell integrity signaling pathway, which is also activated by exposure to heat, osmotic shock, calcofluor white, and Congo red (19, 34, 42, 43, 63). *axl2*Δ colonies were more sensitive to caffeine, high concentrations of Congo red, and high NaCl concentrations than wild-type colonies (Fig. 7B) (sensitivity is defined as an enhanced growth defect beyond the *axl2*Δ growth defect relative to the wild type at 30°C without treatment, which is indicated as a dashed line in Fig. 7B). The loss of Axl2 did not enhance cell wall sensitivity to all stressors, such that for cells exposed to Echinacea, low concentrations of Congo red, and 37°C, growth was diminished to the same degree compared to the wild-type growth as when *axl2*Δ cells were grown without any stresses.

Environmental stresses led to a variety of colony morphology defects. The *axl2*Δ mycelia appeared to be sectored and irregular in comparison to wild-type mycelia under many of these stress-inducing conditions (Fig. 8B). *axl2*Δ cells exposed to 200 μg/ml Congo red appeared to be abnormal in colony shape, and small microcolonies surrounding the central region were visible (Fig. 8A). *axl2*Δ cells grown on 0.2 M NaCl plates displayed alterations in the uniformity of growth, making certain regions of the colony notably thinner or more transparent (Fig. 8B), revealing a sensitivity to low concentrations of NaCl that was not obvious by measuring simply the radial surface area growth. On 0.5 M NaCl plates, both wild-type and *axl2*Δ populations displayed a larger central region of mycelia that did not develop the thickness seen in mycelia grown under no stress, and these colonies grew in an abnormal, asymmetric manner (Fig. 8C). Both wild-type and *axl2*Δ mycelia exposed to 2 mM caffeine developed microcolonies along their surfaces

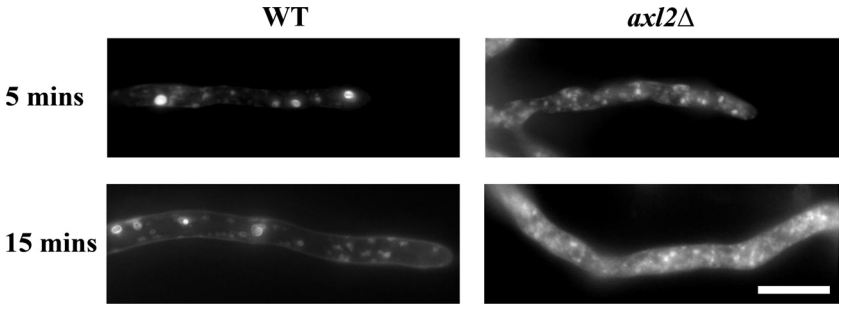

FIG. 5. *axl2*Δ hyphae display a defect in endocytosis. Cells were grown for 16 h at 30°C, followed by growth with FM4-64FX for an additional 5 or 15 min, and fixed with 2% paraformaldehyde. Images were normalized and contrasted to equivalent levels. The scale bar is 10 μm.

and developed yellow mycelia, signifying that caffeine induces riboflavin overproduction (Fig. 8D) (20, 79, 82). Interestingly, while *axl2*Δ mycelia grown with 4 mg/ml Echinacea did not display a radial growth defect, they were clearly abnormal and asymmetric in comparison to wild-type mycelia exposed to identical conditions (Fig. 8E). Many of these treatments disturbing *axl2*Δ surface area growth and mycelium appearance also had some impact on the density (mass/surface area) of these stressed colonies (see Fig. S1A in the supplemental material), with the most substantial effects seen with 20 μg/ml and 200 μg/ml calcofluor white, 200 μg/ml Congo red, 0.5 M NaCl, 2 mM caffeine, and room temperature (see Fig. S1B in the supplemental material).

Environmental stress further depolarizes the *axl2*Δ actin cytoskeleton. To analyze the heat, osmotic, and cell wall sensitivities associated with the *axl2*Δ phenotype, we measured the hyphal tip growth speed, interbranching distance, and actin polarization after treatment with stressors. While exposure to either 37°C or 0.2 M NaCl (at 30°C) decreased the tip growth speed of wild-type hyphae to different levels, both treatments decreased *axl2*Δ hyphal tip growth speeds to similar levels, indicating that this speed may represent a minimal value required to maintain an axis of polarity that is able to promote hyphal elongation (see Fig. S2 in the supplemental material). A branching assay with stress treatments revealed similar results. Exposure to either 37°C, 0.2 M NaCl, 2 mM caffeine, or 200 μg/ml Congo red increased the branching frequency of wild-type cells, with 0.2 M NaCl and 200 μg/ml Congo red having the greatest impact. In contrast, these treatments did not greatly reduce the distance between branches for *axl2*Δ cells (see Fig. S3 in the supplemental material), as these cells may have already attained a maximal branching frequency.

The F-actin cytoskeleton was also visualized after exposure to stressors. Growth at 37°C (Fig. 9A), with 200 μg/ml Congo red (see Fig. S4 in the supplemental material), and with 2 mM caffeine (see Fig. S5 in the supplemental material) all resulted in decreased actin polarization from wild-type hyphal tips, with 200 μg/ml Congo red having the largest impact (Fig. 9B). However, these treatments caused an enhanced actin depolarization in *axl2*Δ cells. Strikingly, these treatments also all caused *axl2*Δ tips to depolarize to very similar levels, again indicating a possible minimal level of actin needed at the tips to maintain hyphal elongation (Fig. 9B and C). However, overall, while heat, osmotic, and cell wall stresses all exacerbated the *axl2*Δ morphological phenotype, mutant cells grown under no stress exhibited the most significant decrease in growth rate and increase in branching frequency relative to wild-type cells.

Axl2 localizes to hyphal tips, branch sites, and septin rings. In order to determine whether Axl2 is present throughout the cell membrane or whether it localizes to specific regions of the hyphae to carry out its roles in polarized growth, we visualized Axl2 by fluorescence microscopy. C-terminal GFP tagging of Axl2 resulted in an aberrant localization throughout the secretory pathway of the hyphae (data not shown). Therefore, we inserted a smaller 6× HA epitope at the C terminus of Axl2. Immunofluorescence revealed Axl2-6HA localization in a cap at hyphal tips, as well as at the cloud of septins that is known to exist at hyphal tips (Fig. 10A). In addition, Axl2 and the septin, Cdc11, were both visualized at branch initiations within the first stages of emergence from the hyphae, and Axl2 was also localized to the branch base of mature branches (Fig. 10B). In some instances, Axl2 was detected at hyphal tips in a thick bar arrangement (Fig. 10C) similar to that seen for newly assembled septin interregion rings (21). Additionally, Axl2 colocalized with mature septin interregion rings (Fig. 10D). Thus, Axl2 is found at sites of polarized growth and septin rings, consistent with *axl2*Δ defects in polarized growth and branching.

DISCUSSION

In budding cells, new polarity axes are formed each cell cycle in nonrandom positions. This requires a network of landmark proteins to mark the spots to establish polarity. In filamentous fungi, the hyphal tip is constitutively polarized and new growth axes emerge as lateral branches that coexist with the growing tip, in some cases in a common cytoplasm with the tip and in other cases in relation to septa. Landmark proteins may function in filamentous cells to stabilize polarized tips, thereby promoting persistent growth, or by directing the location of lateral branch emergence. We find a role for the Axl2 homologue in *Ashbya gossypii* in the maintenance of polarized growth, in the establishment of lateral branches, and in the morphogenetic response to environmental stress. In this way, Axl2 may simultaneously integrate environmental state, cell wall integrity, and morphogenesis to promote optimal hyphal growth.

Axl2 stabilizes polarized growth. *axl2*Δ mutants grow more slowly than the wild type both at the level of the single cell (Fig. 2D and E) and as colonies (Fig. 2C). In addition, we determined that these mutants possess a depolarized actin cytoskeleton (Fig. 4). Actin polarization is necessary for hyphal tip

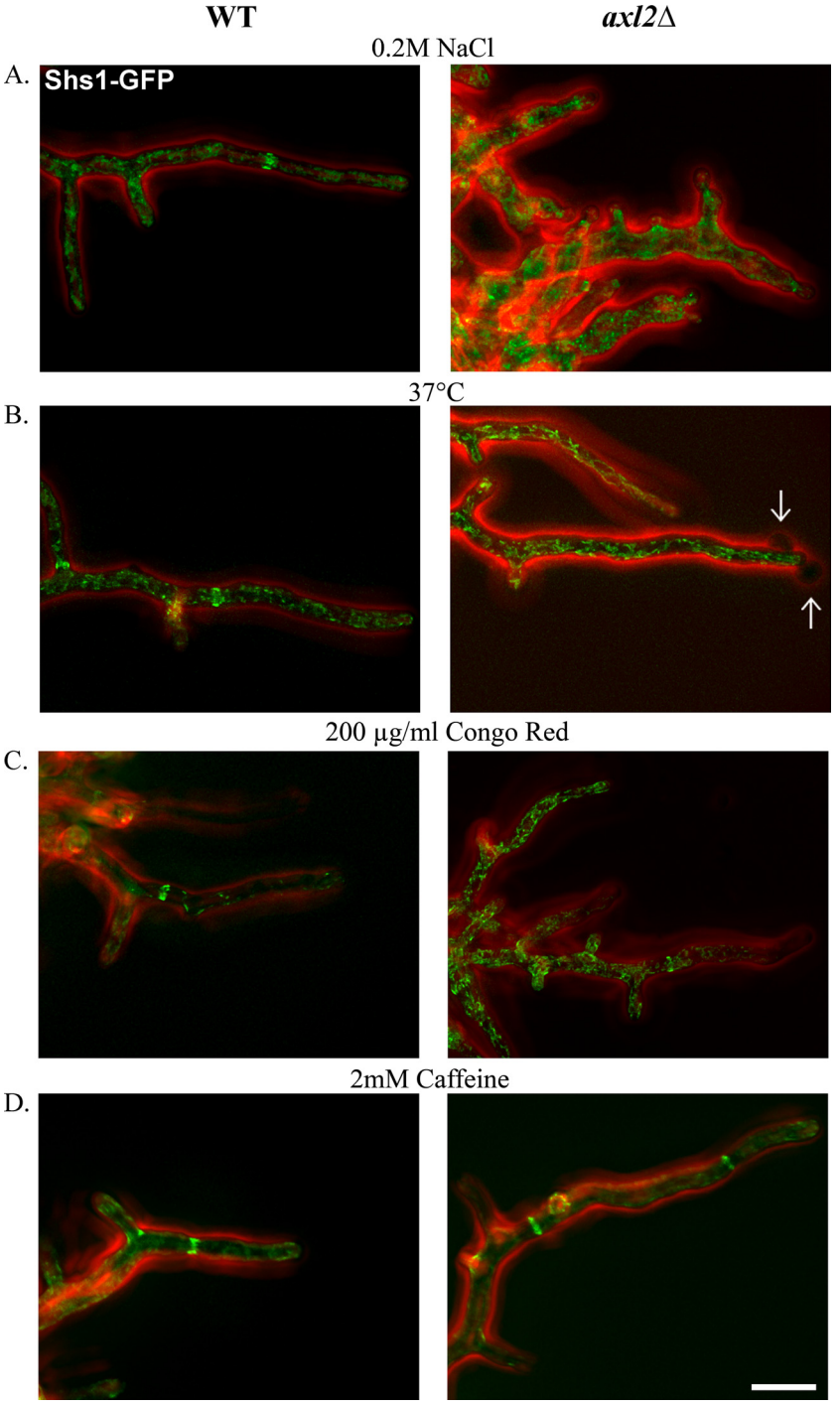

FIG. 6. *axl2*Δ cells are hypersensitive to environmental stress. Cells expressing Shs1-GFP (green) were grown for 15 h at 30°C with 0.2 M NaCl (A), at 37°C (B), at 30°C with 200 μg/ml Congo red (C), or at 30°C with 2 mM caffeine (D) and imaged after fixation with 2% paraformaldehyde. Red represents the phase outline of the cells. Arrows indicate spherical protrusions from hyphae. The scale bar is 10 μm.

growth, and this process is dependent on Cdc42 localization and activation, which itself is dependent on the localization of upstream proteins, such as Cdc24, Rsr1, and Bem1 (2, 44, 99). Axl2 represents a potential upstream protein in this pathway. Axl2 may interact with these proteins, either to recruit them to the hyphal tips or to stabilize and maintain their localization as a complex at the tips. In *S. cerevisiae*, Axl2 is able to interact with Cdc42, Bem1, and Cdc24 (33). It is realistic to hypothesize that such an interaction may play a role in stabilizing this signaling pathway at hyphal tips to allow for maximal initiation and maintenance of actin polarization, leading to concentrated, polarized cell growth through cycles of exocytosis and endocytosis. In the absence of Axl2, both the recruitment and stabilization of Cdc42 at hyphal tips may be disturbed. The

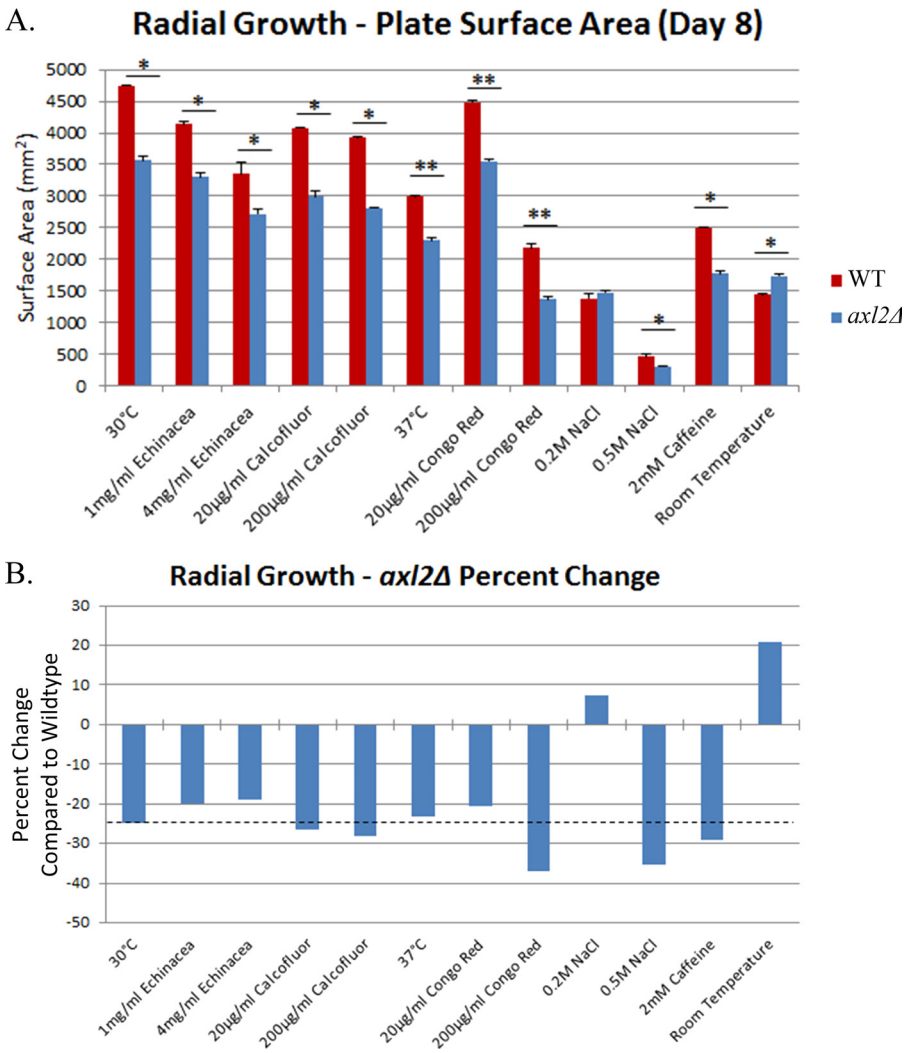

FIG. 7. *axl2*Δ colonies are hypersensitive to environmental stress. (A) Equal concentrations of mycelia were transferred to 85-mm-diameter AFM agarose plates containing the indicated treatment, and mycelium surface areas were measured after 8 days. (B) Values represent the percent change of *axl2*Δ surface area from wild-type surface area with the various treatments. The value of the *axl2*Δ percent change at 30°C with no treatment from Fig. 1C is included and represented by the dashed line. Growth assays were repeated 3 independent times for each strain and condition. Error bars denote standard errors. Statistical significance was determined using two-sample *t* tests with a two-tailed distribution. ∗, $P < 0.05$; ∗∗, $P < 0.001$.

resulting disturbance in the hyphal axis may directly cause the wavy hypha phenotype of *axl2*Δ cells (Fig. 2A).

An additional role of Axl2 in polarized growth may involve endocytosis, a mechanism by which hyphae may restrict the localization of Cdc42 and related polarity markers within the region of polarized growth. Hyphal elongation occurs as vesicles are continually incorporated into the tips. However, this insertion of new membrane will cause existing polarity marker proteins to be pushed outside the hyphal apex unless they are retrieved by endocytosis. New polarity proteins will be incorporated at tips, and the internalized proteins that diffused away from the apex may be recycled through the secretory system (83). In *axl2*Δ cells, cables remained and did not appear to be deformed or depolarized, indicating that normal vesicle transport to tips was likely intact. However, cortical actin patches were severely depolarized, and these cells may be unable to efficiently carry out endocytosis (Fig. 4). Using the fluorescent lipophilic styryl dye FM4-64FX to visualize endocytosis within hyphae, we found an apparent difference in the uptake between the wild type and the *axl2*Δ mutant (Fig. 5). The *axl2*Δ staining pattern is reminiscent of what has been observed in endocytic mutant *S. cerevisiae* and in *S. cerevisiae* exposed to ethanol and heat stress (59, 91). Additionally, a similar phenotype for FM4-64 uptake has been reported for an *Ashbya* mutant lacking Wal1 that also has altered actin patch localization (86). In *axl2*Δ hyphae, efficient exocytosis coupled with inefficient endocytosis may cause polarity markers, such as Cdc42, to migrate outside the hyphal apex, resulting in depolarized, isotropic-like growth and the bulbous tips observed in *axl2*Δ cells (Fig. 2B), as modeled in Fig. S6 in the supplemental material. Other axial bud site landmark proteins have been analyzed in *Aspergillus nidulans*, *Neurospora crassa*, and *Ashbya gossypii*. Bud3 and Bud4 seem to play a conserved role in septal development and maintenance in all three of these systems rather than a direct role in stabilizing polarity (75,

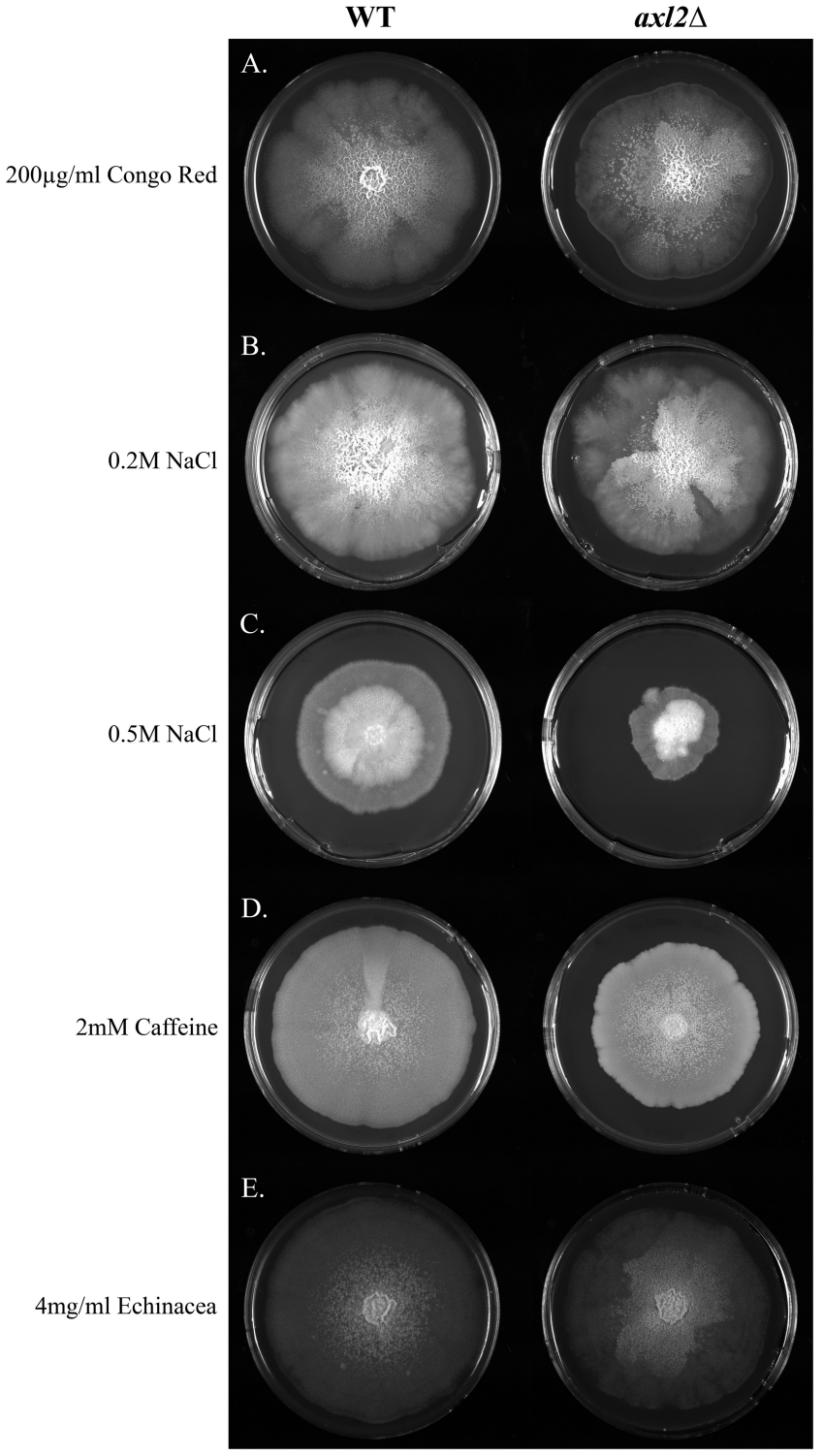

FIG. 8. *axl2*Δ mycelia display abnormal growth patterns after exposure to environmental stress. Equal concentrations of mycelia were transferred to 85-mm-diameter AFM agarose plates containing either 200 μg/ml Congo red (A), 0.2 M NaCl (B), 0.5 M NaCl (C), 2 mM caffeine (D), or 4 mg/ml Echinacea (E). Plates were imaged after colonies either reached the edge of the plate or stopped spreading.

77, 93). In contrast, deletion of the Rsr1/Bud1 homologue in *A. gossypii* causes some phenotypes that are strikingly similar to those of the *axl2*Δ mutants that we report here (8). It may be that in filamentous cells, while the protein interaction network of landmarks that links them to septins or the polarity machinery is conserved, the consequences of these interactions differ from those in yeast and lead to a long-term stabilization of sites of polarity and maturation of septa.

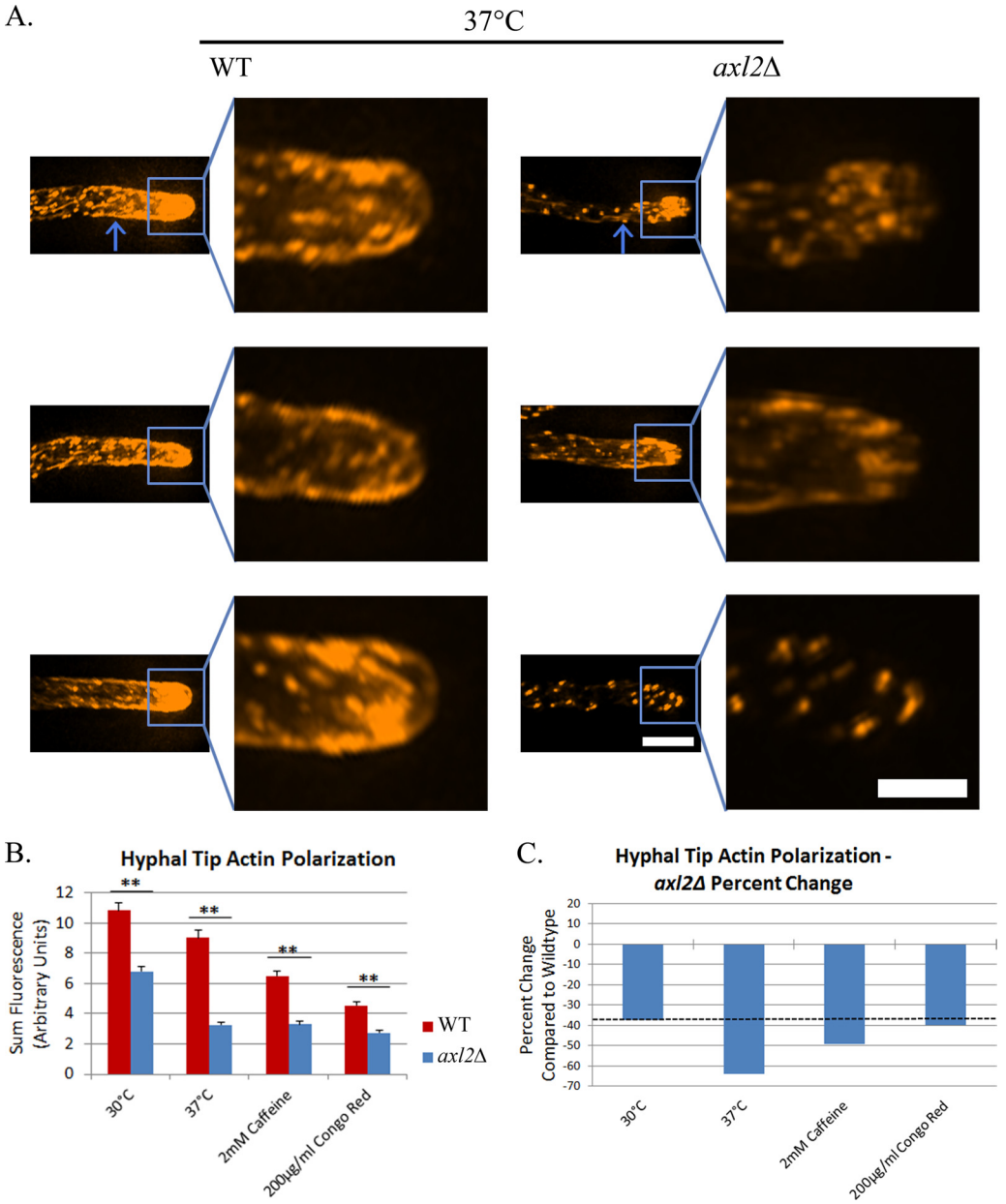

FIG. 9. The *axl2*Δ actin cytoskeleton is hypersensitive to environmental stress. (A) Cells were grown for 16 h either at 37°C or at 30°C with 2 mM caffeine or 200 μg/ml Congo red, and cells were imaged after fixation with 3.7% formaldehyde and actin staining with Alexa Fluor 568 phalloidin. Images of actin fluorescence within hyphae were normalized and contrasted to equivalent levels. Tips were magnified, and actin fluorescence tip images were normalized and contrasted to equivalent levels. Arrows indicate a polarized actin cable. The hypha image bar is 5 μm, and the tip image bar is 2 μm. (B) Sum fluorescence was quantified over an equivalent circular area at hyphal tips. Error bars denote standard errors. Wild type at 37°C, $n = 95$ tips; *axl2*Δ mutant at 37°C, $n = 173$ tips; wild type with 2 mM caffeine, $n = 137$ tips, *axl2*Δ mutant with 2 mM caffeine, $n = 133$ tips; wild type with 200 μg/ml Congo red, $n = 116$ tips; and *axl2*Δ mutant with 200 μg/ml Congo red, $n = 87$ tips. Statistical significance was determined using two-sample *t* tests with a two-tailed distribution. **, $P < 0.001$.

Axl2 as a branch site selection protein. *axl2*Δ cells exhibited an increased branching frequency (Fig. 3C), yet many of these branch events exist as initiations from the hyphae that failed to grow into mature branches (Fig. 3D), causing the decreased density of *axl2*Δ colonies in comparison to wild-type colonies (Fig. 3B). We propose that Axl2 can function as a branch site selection protein to favor branch emergence proximal to septin rings. Axl2 may be recruited to interregion septin rings, which are known to exist in close proximity to branch sites, where it may then function by recruiting specific, currently unknown, branch site initiation proteins (21). Once a minimal branch initiation complex is formed in this region, a branch can emerge. In *axl2*Δ cells, branch site initiation proteins may still be expressed but will no longer be recruited to specific regions along the hyphae. These proteins, now more diffusely dispersed throughout the hyphae, may cause an increase in

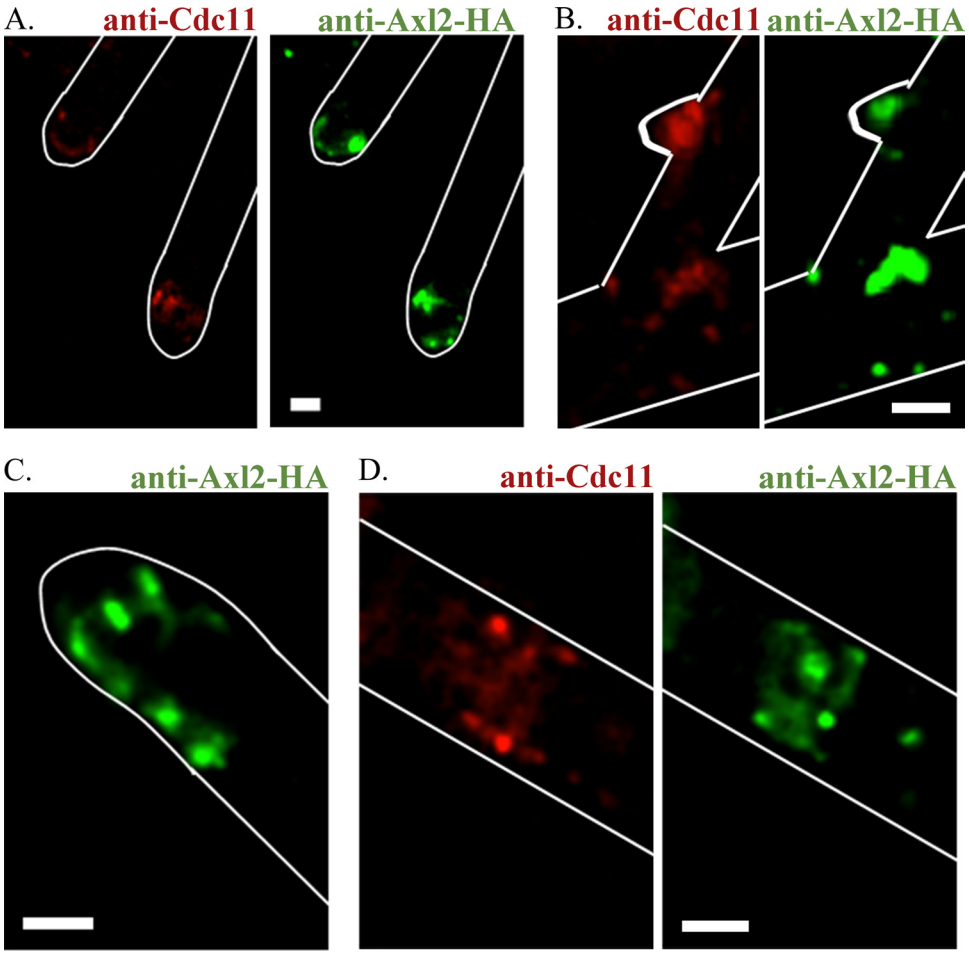

FIG. 10. Axl2-6HA localizes to hyphal tips and branch bases and colocalizes with septin rings. Cells were grown for 16 h at 30°C, fixed with 3.7% formaldehyde, and imaged by immunofluorescence. Images are one Z slice, and the cellular hyphae have been outlined for clarity. (A and B) Both septins and Axl2-6HA were visualized at hyphal tips (A) and bases (B) of both newly emerging and mature branches. (C and D) Axl2 was also localized in a septin bar arrangement at hyphal tips (C) and at interregion septin rings (D). Scale bars are 2 μm.

branch initiations at random locations. This could work potentially via symmetry breaking, a process that allows for polarized growth in the absence of polarity markers through the positive-feedback upregulation of Cdc42 (41). The failure of many of these branches to elongate may be the direct result either of the loss of Axl2 at their tips and a disturbance in polarized growth or of the inability of cells to distribute adequate growth machinery to accommodate an increased number of branches.

Additional evidence indicating that Axl2 is a branch site selection protein is found in comparing *axl2*Δ and wild-type radial growth at room temperature. At this lower temperature, *axl2*Δ colonies grew at a higher rate and were more dense than wild-type colonies (Fig. 7; see Fig. S1 in the supplemental material), in direct opposition to data obtained for *axl2*Δ and wild-type colonies grown at 30°C. At this lower, less stressful temperature, *axl2*Δ hyphae may be able to overcome some level of the polarization defect exhibited at 30°C. However, these cells may still continue to experience an increased branching frequency, leading to an increased number of elongating hyphae and increasing the overall *axl2*Δ colony radial growth and density in comparison to those of wild-type colonies.

Axl2 as a cell wall integrity protein. The *axl2*Δ mutant displayed an increased sensitivity to Congo red, caffeine, heat, and NaCl (Fig. 6, 7, and 8), all of which are known to disturb the cell wall. In *A. gossypii*, unlike in *S. cerevisiae*, Axl2 contains a predicted Mid2 homology domain. ScMid2 functions as a cell wall stress sensor and signals through ScRom2, the ScRho1 GEF, to cause cell wall remodeling and repair in response to the stress (64, 68). In *A. gossypii*, Axl2 may play a role similar to that of ScMid2 in budding yeast. *axl2*Δ cells may no longer be able to sense stress and propagate the necessary signal to intracellular cell wall-remodeling proteins.

Under cell wall stress, *axl2*Δ cells display morphological deformities that resemble an exacerbation of the *axl2*Δ phenotype under no stress (Fig. 6). Stressed *axl2*Δ cells displayed an increase in the severity of hyphal "waviness," branch initiations that failed to elongate, and bulbous tip deformities. These cells lack a protein that we have demonstrated is important for polarized growth at hyphal tips, the most vulnerable part of the cell, where elongation and membrane remodeling are constantly occurring. Under stress, this region is being further exploited and polarized growth further hampered, consistent

with both the exacerbated morphological phenotype and the increased actin depolarization of *axl2*Δ cells. Axl2 in *A. gossypii*, like its homologue in *S. cerevisiae*, may contain N-linked and O-linked glycosylations. Axl2 may therefore function in maintaining cell wall integrity through a direct, physical interaction in linking the plasma membrane to the cell wall.

It is also possible that the loss of Axl2 disturbs other signaling pathways. The vulnerability of *axl2*Δ mutants to heat and osmotic stress may be due not only to their cell wall sensitivity but also to a disturbance in pathways such as the conserved high-osmolarity glycerol (HOG) mitogen-activated protein kinase (MAPK) signaling pathway, which is activated after exposure to both heat and NaCl (95, 96). In addition, the *axl2*Δ mutant's sensitivity to caffeine might not be directly due to caffeine's role as a cell wall disturber. Caffeine, similarly to the antibiotic rapamycin, has also been shown to be an inhibitor of the yeast TOR1/2 pathway, which is important for determining cell growth in response to sensing environmental nutrients (51, 53). We have observed that wild-type mycelia, but not *axl2*Δ mycelia, are able to grow on plates containing 200 nM rapamycin (data not shown). Axl2 may be required for different pathways necessary for responding to various stressors. The addition of the Mid2 homology to this polarity-stabilizing protein may serve to integrate morphogenesis with the stress response.

In summary, we report a multifunctional role of Axl2 in cell polarity initiation, maintenance, and growth in the face of environmental stress. The integration of these diverse functions in a single protein may be an important mode for filamentous fungi to maintain and establish multiple, persistent axes of polarized growth in a single cell.

ACKNOWLEDGMENTS

We thank Rebecca Meseroll for early support of the project, Cori D'Ausilio for assistance in image processing, and members of the Gladfelter lab for useful discussions.

This work was supported by an NSF grant to A.S.G. (MCB MCB-0719126) and a Dean of the College Undergraduate Research Award from Dartmouth College to J.F.A.

REFERENCES

1. **Adames, N., K. Blundell, M. N. Ashby, and C. Boone.** 1995. Role of yeast insulin-degrading enzyme homologs in propheromone processing and bud site selection. Science **270:**464–467.
2. **Adams, A. E., D. I. Johnson, R. M. Longnecker, B. F. Sloat, and J. R. Pringle.** 1990. CDC42 and CDC43, two additional genes involved in budding and the establishment of cell polarity in the yeast Saccharomyces cerevisiae. J. Cell Biol. **111:**131–142.
3. **Almeida, A. J., et al.** 2009. Cdc42p controls yeast-cell shape and virulence of Paracoccidioides brasiliensis. Fungal Genet. Biol. **46:**919–926.

3a. **Altmann-Jöhl, R., and P. Philippsen.** 1996. AgTHR4, a new selection marker for transformation of the filamentous fungus *Ashbya gossypii*, maps in a four-gene cluster that is conserved between *A. gossypii* and *Saccharomyces cerevisiae*. Mol. Gen. Genet. **250:**69–80.

4. **Ayad-Durieux, Y., P. Knechtle, S. Goff, F. Dietrich, and P. Philippsen.** 2000. A PAK-like protein kinase is required for maturation of young hyphae and septation in the filamentous ascomycete Ashbya gossypii. J. Cell Sci. **113:** 4563–4575.
5. **Baas, P. W., M. M. Black, and G. A. Banker.** 1989. Changes in microtubule polarity orientation during the development of hippocampal neurons in culture. J. Cell Biol. **109:**3085–3094.
6. **Bachewich, C., A. Nantel, and M. Whiteway.** 2005. Cell cycle arrest during S or M phase generates polarized growth via distinct signals in Candida albicans. Mol. Microbiol. **57:**942–959.
7. **Barral, Y., V. Mermall, M. S. Mooseker, and M. Snyder.** 2000. Compartmentalization of the cell cortex by septins is required for maintenance of cell polarity in yeast. Mol. Cell **5:**841–851.
8. **Bauer, Y., P. Knechtle, J. Wendland, H. Helfer, and P. Philippsen.** 2004. A Ras-like GTPase is involved in hyphal growth guidance in the filamentous fungus Ashbya gossypii. Mol. Biol. Cell **15:**4622–4632.
9. **Bouquin, N., et al.** 2000. Regulation of cytokinesis by the Elm1 protein kinase in Saccharomyces cerevisiae. J. Cell Sci. **113:**1435–1445.
10. **Brachat, S., et al.** 2003. Reinvestigation of the Saccharomyces cerevisiae genome annotation by comparison to the genome of a related fungus: Ashbya gossypii. Genome Biol. **4:**R45.
11. **Bretscher, A., B. Drees, E. Harsay, D. Schott, and T. Wang.** 1994. What are the basic functions of microfilaments? Insights from studies in budding yeast. J. Cell Biol. **126:**821–825.
12. **Caviston, J. P., M. Longtine, J. R. Pringle, and E. Bi.** 2003. The role of Cdc42p GTPase-activating proteins in assembly of the septin ring in yeast. Mol. Biol. Cell **14:**4051–4066.
13. **Cerveira, N., J. Santos, and M. R. Teixeira.** 2009. Structural and expression changes of septins in myeloid neoplasia. Crit. Rev. Oncogenesis **15:**91–115.
14. **Chant, J., M. Mischke, E. Mitchell, I. Herskowitz, and J. R. Pringle.** 1995. Role of Bud3p in producing the axial budding pattern of yeast. J. Cell Biol. **129:**767–778.
15. **Cheon, M. S., M. Fountoulakis, M. Dierssen, J. C. Ferreres, and G. Lubec.** 2001. Expression profiles of proteins in fetal brain with Down syndrome. J. Neural Transm. Suppl. **2001:**311–319.
16. **Cho, R. J., et al.** 1998. A genome-wide transcriptional analysis of the mitotic cell cycle. Mol. Cell **2:**65–73.
17. **Chowdhury, S., K. W. Smith, and M. C. Gustin.** 1992. Osmotic stress and the yeast cytoskeleton: phenotype-specific suppression of an actin mutation. J. Cell Biol. **118:**561–571.
18. **Cvrcková, F., C. De Virgilio, E. Manser, J. R. Pringle, and K. Nasmyth.** 1995. Ste20-like protein kinases are required for normal localization of cell growth and for cytokinesis in budding yeast. Genes Dev. **9:**1817–1830.
19. **Davenport, K. R., M. Sohaskey, Y. Kamada, D. E. Levin, and M. C. Gustin.** 1995. A second osmosensing signal transduction pathway in yeast. Hypotonic shock activates the PKC1 protein kinase-regulated cell integrity pathway. J. Biol. Chem. **270:**30157–30161.
20. **Demain, A. L.** 1972. Riboflavin oversynthesis. Annu. Rev. Microbiol. **26:**369–388.
21. **DeMay, B. S., R. A. Meseroll, P. Occhipinti, and A. S. Gladfelter.** 2009. Regulation of distinct septin rings in a single cell by Elm1p and Gin4p kinases. Mol. Biol. Cell **20:**2311–2326.
22. **Desrivieres, S., F. T. Cooke, P. J. Parker, and M. N. Hall.** 1998. MSS4, a phosphatidylinositol-4-phosphate 5-kinase required for organization of the actin cytoskeleton in Saccharomyces cerevisiae. J. Biol. Chem. **273:**15787–15793.
23. **Dickens, N. J., S. Beatson, and C. P. Ponting.** 2002. Cadherin-like domains in alpha-dystroglycan, alpha/epsilon-sarcoglycan and yeast and bacterial proteins. Curr. Biol. **19:**R197–R199.
24. **Dietrich, F. S., et al.** 2004. The Ashbya gossypii genome as a tool for mapping the ancient Saccharomyces cerevisiae genome. Science **304:**304–307.
25. **Drubin, D. G., and W. J. Nelson.** 1996. Origins of cell polarity. Cell **84:**335–344.
26. **Elorza, M. V., H. Rico, and R. Sentandreu.** 1983. Calcofluor white alters the assembly of chitin fibrils in Saccharomyces cerevisiae and Candida albicans cells. J. Gen. Microbiol. **129:**1577–1582.
27. **Field, C. M., and D. Kellogg.** 1999. Septins: cytoskeletal polymers or signalling GTPases? Trends Cell Biol. **9:**387–394.
28. **Finger, F. P., K. R. Kopish, and J. G. White.** 2003. A role for septins in cellular and axonal migration in C. elegans. Dev. Biol. **261:**220–234.
29. **Finger, F. P., and P. Novick.** 1998. Spatial regulation of exocytosis: lessons from yeast. J. Cell Biol. **142:**609–612.
30. **Flescher, E. G., K. Madden, and M. Snyder.** 1993. Components required for cytokinesis are important for bud site selection in yeast. J. Cell Biol. **122:** 373–386.
31. **Fujita, A., et al.** 1994. A yeast gene necessary for bud-site selection encodes a protein similar to insulin-degrading enzymes. Nature **372:**567–570.
32. **Fujita, A., et al.** 2004. Rax1, a protein required for the establishment of the bipolar budding pattern in yeast. Gene **327:**161–169.
33. **Gao, X.-D., et al.** 2007. Sequential and distinct roles of the cadherin domain-containing protein Axl2p in cell polarization in yeast cell cycle. Mol. Biol. Cell **18:**2542–2560.
34. **García, R., et al.** 2004. The global transcriptional response to transient cell wall damage in Saccharomyces cerevisiae and its regulation by the cell integrity signaling pathway. J. Biol. Chem. **279:**15183–15195.
35. **Gladfelter, A. S., J. R. Pringle, and D. J. Lew.** 2001. The septin cortex at the yeast mother-bud neck. Curr. Opin. Microbiol. **4:**681–689.
36. **Goodson, H. V., B. L. Anderson, H. M. Warrick, L. A. Pon, and J. A. Spudich.** 1996. Synthetic lethality screen identifies a novel yeast myosin I gene (MYO5): myosin I proteins are required for polarization of the actin cytoskeleton. J. Cell Biol. **133:**1277–1291.
37. **Govindan, B., R. Bowser, and P. Novick.** 1995. The role of Myo2, a yeast class V myosin, in vesicular transport. J. Cell Biol. **128:**1055–1068.
38. **Halme, A., M. Michelitch, E. L. Mitchell, and J. Chant.** 1996. Bud10p directs axial cell polarization in budding yeast and resembles a transmembrane receptor. Curr. Biol. **6:**570–579.
39. **Harold, F. M.** 1995. From morphogenes to morphogenesis. Microbiology **141:**2765–2778.
40. **Imai, K., Y. Noda, H. Adachi, and K. Yoda.** 2005. A novel endoplasmic

reticulum membrane protein Rcr1 regulates chitin deposition in the cell wall of Saccharomyces cerevisiae. J. Biol. Chem. **280:**8275–8284.
41. **Irazoqui, J. E., A. S. Gladfelter, and D. J. Lew.** 2003. Scaffold-mediated symmetry breaking by Cdc42p. Nat. Cell Biol. **5:**1062–1070.
42. **Jacoby, J. J., S. M. Nilius, and J. J. Heinisch.** 1998. A screen for upstream components of the yeast protein kinase C signal transduction pathway identifies the product of the SLG1 gene. Mol. Gen. Genet. **258:**148–155.
43. **Kamada, Y., U. S. Jung, J. Piotrowski, and D. E. Levin.** 1995. The protein kinase C-activated MAP kinase pathway of Saccharomyces cerevisiae mediates a novel aspect of the heat shock response. Genes Dev. **9:**1559–1571.
44. **Kang, P. J., A. Sanson, B. Lee, and H. O. Park.** 2001. A GDP/GTP exchange factor involved in linking a spatial landmark to cell polarity. Science **292:** 1376–1378.
45. **Kang, P. J., B. Lee, and H.-O. Park.** 2004. Specific residues of the GDP/GTP exchange factor Bud5p are involved in establishment of the cell type-specific budding pattern in yeast. J. Biol. Chem. **279:**27980–27985.
46. **Kartmann, B., and D. Roth.** 2001. Novel roles for mammalian septins: from vesicle trafficking to oncogenesis. J. Cell Sci. **114:**839–844.
47. **Kinoshita, A., et al.** 1998. Identification of septins in neurofibrillary tangles in Alzheimer's disease. Am. J. Pathol. **153:**1551–1560.
48. **Knechtle, P., F. Dietrich, and P. Philippsen.** 2003. Maximal polar growth potential depends on the polarisome component AgSpa2 in the filamentous fungus Ashbya gossypii. Mol. Biol. Cell **14:**4140–4154.
49. **Köhli, M., V. Galati, K. Boudier, R. W. Roberson, and P. Philippsen.** 2008. Growth-speed-correlated localization of exocyst and polarisome components in growth zones of Ashbya gossypii hyphal tips. J. Cell Sci. **121:**3878–3889.
50. **Kopecká, M., and M. Gabriel.** 1992. The influence of Congo red on the cell wall and (1-3)-beta-D-glucan microfibril biogenesis in Saccharomyces cerevisiae. Arch. Microbiol. **158:**115–126.
51. **Kuranda, K., V. Leberre, S. Sokol, G. Palamarczyk, and J. François.** 2006. Investigating the caffeine effects in the yeast Saccharomyces cerevisiae brings new insights into the connection between TOR, PKC and Ras/cAMP signalling pathways. Mol. Microbiol. **61:**1147–1166.
52. **Lillie, S. H., and S. S. Brown.** 1994. Immunofluorescence localization of the unconventional myosin, Myo2p, and the putative kinesin-related protein, Smy1p, to the same regions of polarized growth in Saccharomyces cerevisiae. J. Cell Biol. **125:**825–842.
53. **Loewith, R., et al.** 2002. Two TOR complexes, only one of which is rapamycin sensitive, have distinct roles in cell growth control. Mol. Cell **10:**457–468.
54. **Longtine, M. S., H. Fares, and J. R. Pringle.** 1998. Role of the yeast Gin4p protein kinase in septin assembly and the relationship between septin assembly and septin function. J. Cell Biol. **143:**719–736.
55. **Lord, M., et al.** 2002. Subcellular localization of Axl1, the cell type-specific regulator of polarity. Curr. Biol. **12:**1347–1352.
56. **Lord, M., M. C. Yang, M. Mischke, and J. Chant.** 2000. Cell cycle programs of gene expression control morphogenetic protein localization. J. Cell Biol. **151:**1501–1512.
57. **Madania, A., et al.** 1999. The Saccharomyces cerevisiae homologue of human Wiskott-Aldrich syndrome protein Las17p interacts with the Arp2/3 complex. Mol. Biol. Cell **10:**3521–3538.
58. **Matsui, Y., and A. Toh-e.** 1992. Yeast RHO3 and RHO4 ras superfamily genes are necessary for bud growth, and their defect is suppressed by a high dose of bud formation genes CDC42 and BEM1. Mol. Cell. Biol. **12:**5690–5699.
59. **Meaden, P. G., N. Arneborg, L. U. Guldfeldt, H. Siegumfeldt, and M. Jakobsen.** 1999. Endocytosis and vacuolar morphology in Saccharomyces cerevisiae are altered in response to ethanol stress or heat shock. Yeast **15:**1211–1222.
60. **Mir-Rashed, N., et al.** 2010. Disruption of fungal cell wall by antifungal Echinacea extracts. Int. Soc. Hum. Anim. Mycol. **48:**949–958.
61. **Mulholland, J., A. Wesp, H. Riezman, and D. Botstein.** 1997. Yeast actin cytoskeleton mutants accumulate a new class of Golgi-derived secretary vesicle. Mol. Biol. Cell **8:**1481–1499.
62. **Park, H.-O., and E. Bi.** 2007. Central roles of small GTPases in the development of cell polarity in yeast and beyond. Microbiol. Mol. Biol. Rev. **71:**48–96.
63. **Park, J.-I., E. J. Collinson, C. M. Grant, and I. W. Dawes.** 2005. Rom2p, the Rho1 GTP/GDP exchange factor of Saccharomyces cerevisiae, can mediate stress responses via the Ras-cAMP pathway. J. Biol. Chem. **280:**2529–2535.
64. **Philip, B., and D. E. Levin.** 2001. Wsc1 and Mid2 are cell surface sensors for cell wall integrity signaling that act through Rom2, a guanine nucleotide exchange factor for Rho1. Mol. Cell. Biol. **21:**271–280.
65. **Powers, J., and C. Barlowe.** 2002. Erv14p directs a transmembrane secretory protein into COPII-coated transport vesicles. Mol. Biol. Cell **13:**880–891.
66. **Powers, J., and C. Barlowe.** 1998. Transport of axl2p depends on erv14p, an ER-vesicle protein related to the Drosophila cornichon gene product. J. Cell Biol. **142:**1209–1222.
67. **Price, M. S., C. B. Nichols, and J. A. Alspaugh.** 2008. The Cryptococcus neoformans Rho-GDP dissociation inhibitor mediates intracellular survival and virulence. Infect. Immun. **76:**5729–5737.
68. **Rajavel, M., B. Philip, B. M. Buehrer, B. Errede, and D. E. Levin.** 1999. Mid2 is a putative sensor for cell integrity signaling in Saccharomyces cerevisiae. Mol. Cell. Biol. **19:**3969–3976.
69. **Roemer, T., K. Madden, J. Chang, and M. Snyder.** 1996. Selection of axial growth sites in yeast requires Axl2p, a novel plasma membrane glycoprotein. Genes Dev. **10:**777–793.
70. **Roncero, C., and A. Durán.** 1985. Effect of calcofluor white and Congo red on fungal cell wall morphogenesis: in vivo activation of chitin polymerization. J. Bacteriol. **163:**1180–1185.
71. **Roncero, C., M. H. Valdivieso, J. C. Ribas, and A. Durán.** 1988. Effect of calcofluor white on chitin synthases from Saccharomyces cerevisiae. J. Bacteriol. **170:**1945–1949.
72. **Sanders, S. L., and I. Herskowitz.** 1996. The BUD4 protein of yeast, required for axial budding, is localized to the mother/BUD neck in a cell cycle-dependent manner. J. Cell Biol. **134:**413–427.
73. **Sanders, S. L., M. Gentzsch, W. Tanner, and I. Herskowitz.** 1999. O-Glycosylation of Axl2/Bud10p by Pmt4p is required for its stability, localization, and function in daughter cells. J. Cell Biol. **145:**1177–1188.
74. **Schmitz, H.-P., A. Kaufmann, M. Köhli, P. P. Laissue, and P. Philippsen.** 2006. From function to shape: a novel role of a formin in morphogenesis of the fungus Ashbya gossypii. Mol. Biol. Cell. **17:**130–145.
75. **Seiler, S., and D. Justa-Schuch.** 2010. Conserved components, but distinct mechanisms for the placement and assembly of the cell division machinery in unicellular and filamentous ascomycetes. Mol. Microbiol. **78:**1058–1076.
76. **Shemluck, M.** 1982. Medicinal and other uses of the Compositae by Indians in the United States and Canada. J. Ethnopharmacol. **5:**303–358.
77. **Si, H., D. Justa-Schuch, S. Seiler, and S. D. Harris.** 2010. Regulation of septum formation by the Bud3-Rho4 GTPase module in Aspergillus nidulans. Genetics **185:**165–176.
78. **Spellman, P. T., et al.** 1998. Comprehensive identification of cell cycle-regulated genes of the yeast Saccharomyces cerevisiae by microarray hybridization. Mol. Biol. Cell **9:**3273–3297.
79. **Stahmann, K. P., J. L. Revuelta, and H. Seulberger.** 2000. Three biotechnical processes using Ashbya gossypii, Candida famata, or Bacillus subtilis compete with chemical riboflavin production. Appl. Microbiol. Biotechnol. **53:**509–516.
80. **Steinbach, W. J., et al.** 2006. Calcineurin controls growth, morphology, and pathogenicity in Aspergillus fumigatus. Eukaryot. Cell **5:**1091–1103.
81. **Takizawa, P. A., J. L. DeRisi, J. E. Wilhelm, and R. D. Vale.** 2000. Plasma membrane compartmentalization in yeast by messenger RNA transport and a septin diffusion barrier. Science **290:**341–344.
82. **Tanner, F. W., and J. M. Van Lanen.** 1947. Riboflavin production by Ashbya gossypii. J. Bacteriol. **54:**38.
83. **Upadhyay, S., and B. D. Shaw.** 2008. The role of actin, fimbrin and endocytosis in growth of hyphae in Aspergillus nidulans. Mol. Microbiol. **68:**690–705.
84. **Versele, M., and J. Thorner.** 2004. Septin collar formation in budding yeast requires GTP binding and direct phosphorylation by the PAK, Cla4. J. Cell Biol. **164:**701–715.
85. **Versele, M., and J. Thorner.** 2005. Some assembly required: yeast septins provide the instruction manual. Trends Cell Biol. **15:**414–424.
86. **Walther, A., and J. Wendland.** 2004. Apical localization of actin patches and vacuolar dynamics in Ashbya gossypii depend on the WASP homolog Wal1p. J. Cell Sci. **117:**4947–4958.
87. **Warenda, A. J., S. Kauffman, T. P. Sherrill, J. M. Becker, and J. B. Konopka.** 2003. Candida albicans septin mutants are defective for invasive growth and virulence. Infect. Immun. **71:**4045–4051.
88. **Weiner, O. D.** 2002. Regulation of cell polarity during eukaryotic chemotaxis: the chemotactic compass. Curr. Opin. Cell Biol. **14:**196–202.
89. **Weirich, C. S., J. P. Erzberger, and Y. Barral.** 2008. The septin family of GTPases: architecture and dynamics. Nat. Rev. Mol. Cell Biol. **9:**478–489.
90. **Weiss, E. L., A. C. Bishop, K. M. Shokat, and D. G. Drubin.** 2000. Chemical genetic analysis of the budding-yeast p21-activated kinase Cla4p. Nat. Cell Biol. **2:**677–685.
91. **Wendland, B., J. M. McCaffery, Q. Xiao, and S. D. Emr.** 1996. A novel fluorescence-activated cell sorter-based screen for yeast endocytosis mutants identifies a yeast homologue of mammalian eps15. J. Cell Biol. **135:**1485–1500.
92. **Wendland, J., Y. Ayad-Durieux, P. Knechtle, C. Rebischung, and P. Philippsen.** 2000. PCR-based gene targeting in the filamentous fungus Ashbya gossypii. Gene **242:**381–391.
93. **Wendland, J.** 2003. Analysis of the landmark protein Bud3 of Ashbya gossypii reveals a novel role in septum construction. EMBO Rep. **4:**200–204.
94. **Wendland, J., and A. Walther.** 2005. Ashbya gossypii: a model for fungal developmental biology. Nat. Rev. Microbiol. **3:**421–429.
95. **Winkler, A., et al.** 2002. Heat stress activates the yeast high-osmolarity glycerol mitogen-activated protein kinase pathway, and protein tyrosine phosphatases are essential under heat stress. Eukaryot. Cell **1:**163–173.
96. **Wu, X., et al.** 2010. The evolutionary rate variation among genes of HOG-signaling pathway in yeast genomes. Biol. Direct. **5:**46.
97. **Zegers, M. M., and D. Hoekstra.** 1998. Mechanisms and functional features of polarized membrane traffic in epithelial and hepatic cells. Biochem. J. **336:**257–269.
98. **Zheng, Y., A. Bender, and R. A. Cerione.** 1995. Interactions among proteins involved in bud-site selection and bud-site assembly in Saccharomyces cerevisiae. J. Biol. Chem. **270:**626–630.
99. **Ziman, M., et al.** 1993. Subcellular localization of Cdc42p, a Saccharomyces cerevisiae GTP-binding protein involved in the control of cell polarity. Mol. Biol. Cell **4:**1307–1316.